Novel Maximum-Power-Point-Tracking Controller for Photovoltaic Energy Conversion System

Yeong-Chau Kuo, Tsorng-Juu Liang, *Member, IEEE*, and Jiann-Fuh Chen, *Member, IEEE*

***Abstract*—A novel maximum-power-point-tracking (MPPT) controller for a photovoltaic (PV) energy conversion system is presented. Using the slope of power versus voltage of a PV array, the proposed MPPT controller allows the conversion system to track the maximum power point very rapidly. As opposed to conventional two-stage designs, a single-stage configuration is implemented, resulting in size and weight reduction and increased efficiency. The proposed system acts as a solar generator on sunny days, in addition to working as an active power line conditioner on rainy days. Finally, computer simulations and experimental results demonstrate the superior performance of the proposed technique.**

***Index Terms*—Active power line conditioner, maximum-power-point tracking, photovoltaic energy conversion system, solar generator.**

I. Introduction

PHOTOVOLTAIC (PV) energy is the most important energy resource since it is clean, pollution free, and inexhaustible. Due to rapid growth in the semiconductor and power electronics techniques, PV energy is of increasing interest in electrical power applications. It is important to operate PV energy conversion systems near the maximum power point to increase the output efficiency of PV arrays. Therefore, many techniques have been developed to provide maximum PV power [1]–[10]. Enslin employed an integrated PV maximum-power-point tracker with soft switching to obtain the optimum efficiency [1]. Hiyama used a neural network to estimate maximum-power-point operating conditions [2], [3]. Some researchers control photovoltaic characteristics to match load conditions [4]–[6]. Some systems use an online maximum power point tracking (MPPT) algorithm to obtain the maximum power point [7]–[10]. An MPPT method often used is the perturbation and observation method [8], [9], because the method is easy to implement. However, oscillation is unavoidable. The incremental conductance method is used to avoid oscillation by comparing the incremental and instantaneous conductance of the PV array, but the implemented circuit is more complex [10]. In this paper, using the slope of power versus voltage, a novel MPPT algorithm is presented which avoids the oscillation problem and is easy to implement.

Conventionally, PV energy conversion systems are composed of a dc/dc converter, a dc/ac inverter, batteries, and a center-tapped output transformer [11]–[13]. The efficiency of such series-connected multistage devices is low. Further, the size is large and the weight is high. The proposed design, by contrast, uses a single-stage configuration, thus increasing efficiency and reducing size. In addition, the proposed system operates as power supply on sunny days and operates as an active power line conditioner at low or zero insolation. Hence, the proposed PV energy conversion system provides useful function in any weather, significantly enhancing system utility.

Manuscript received February 27, 2000; revised January 25, 2001. Abstract published on the Internet February 15, 2001.

The authors are with the Department of Electrical Engineering, National Cheng Kung University, Tainan 701, Taiwan, R.O.C. (e-mail: Chenjf@mail.ncku.edu.tw; tjliang@mail.ncku.edu.tw).

Publisher Item Identifier S 0278-0046(01)03812-6.

II. Proposed MPPT Algorithm

Fig. 1(a) depicts the output characteristics of a PV array, where V and P are output voltage and power of the PV array, respectively. The output power of the PV array is expressed as

$$P = VI. \tag{1}$$

The conventional MPPT algorithms use $dP/dV = 0$ to obtain the maximum output power point. The perturbation and observation method measures ΔP and ΔV to judge the momentary operating region, and then, according to the region, the reference voltage is increased or decreased such that the systems operates close to the maximum power point. Because the method increases or decreases only the reference voltage, implementation is simple. However, the method cannot readily track immediate and rapid changes in environmental conditions. An alternative method, the incremental conductance method, tracks the maximum power point accurately by comparing the incremental conductance and instantaneous conductance of a PV array [10].

If the internal shunt resistance is neglected, the characteristic of a PV array can be given as [8], [9]

$$I = I_g - I_{\text{sat}} \left\{ \exp\left[\frac{q}{AKT}(V + IR_s) \right] - 1 \right\} \tag{2}$$

where

- I_g light-generated current;
- I_{sat} PV array saturation current;
- q charge of an electron;
- K Boltzmann's constant;
- A ideality factor of the p–n junction;
- T PV array temperature (K);
- R_s intrinsic series resistance of the PV array.

Since the series resistance R_s can be neglected, (2) can be simplified as

$$I = I_g - I_{\text{sat}} \left[\exp\left(\frac{qV}{AKT} \right) - 1 \right]. \tag{3}$$

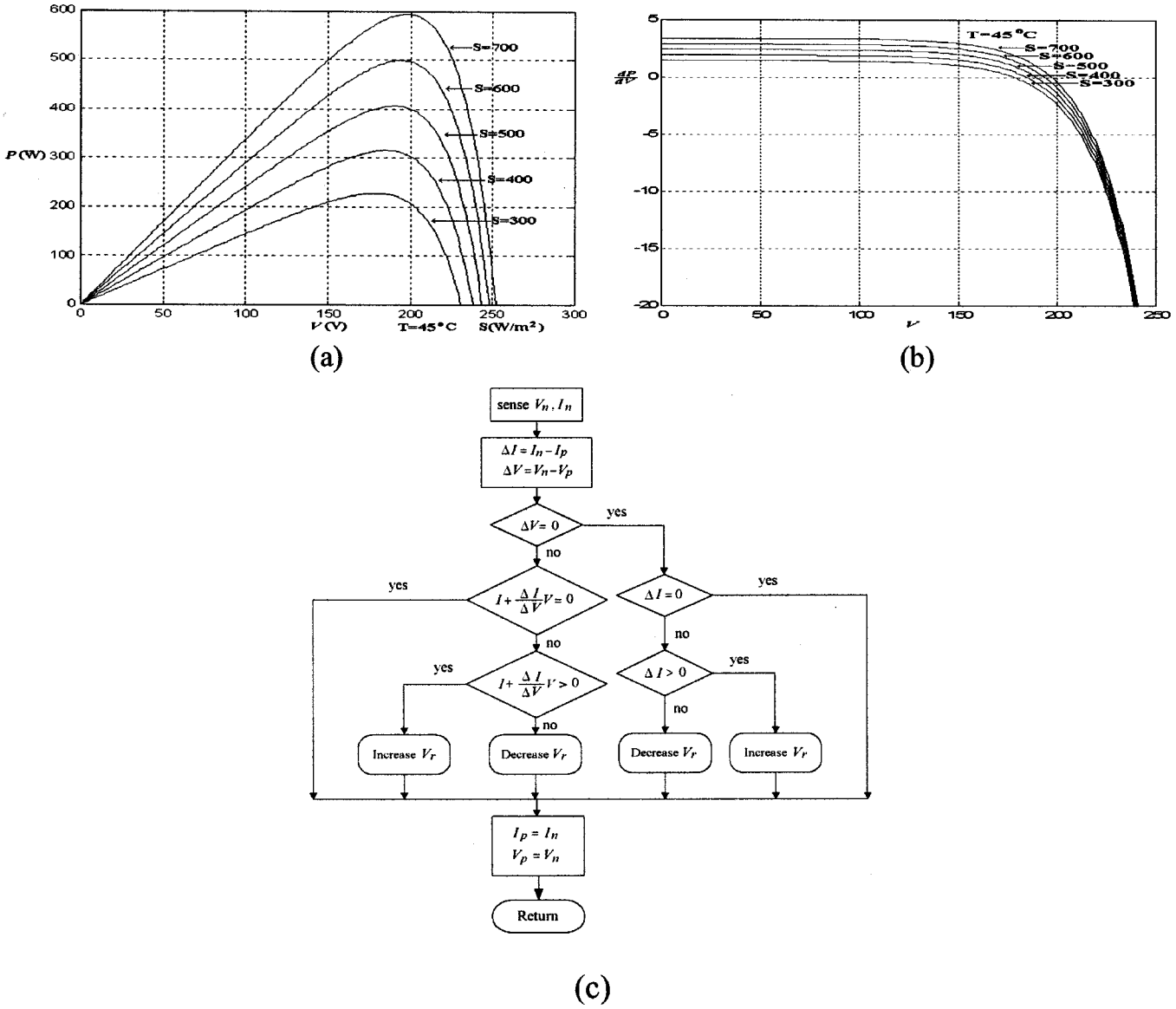

Fig. 1. (a) Characteristic diagram of P versus V. (b) Diagram of dP/dV versus V. (c) Flowchart of the proposed method.

From (1) and (3), the differential of P to V can be expressed as

$$\frac{dP}{dV} = I + \frac{dI}{dV}V = I_g - I_{\text{sat}}\left[\exp\left(\frac{qV}{AKT}\right) - 1\right] - \frac{qI_{\text{sat}}}{AKT}\exp\left(\frac{qV}{AKT}\right)V \tag{4}$$

$$\frac{dP}{dV} \cong I + \frac{\Delta I}{\Delta V}V \tag{5}$$

where ΔI and ΔV are the increments of output voltage and current, respectively. Equation (4) is the function of V that can be employed to simulate the characteristic of dP/dV versus V, and the result is shown in Fig. 1(b). From (5), the dP/dV term can be replaced by $I + (\Delta I/\Delta V)V$, making the calculation practical for an 89c51 microprocessor. In the proposed method, (5) is used as the index of the MPPT operation. The calculation of (5) requires only one division and one multiplication instruction, which is easier than the incremental conductance method.

Fig. 1(b) depicts the diagram of dP/dV versus V when the insolation is varied from 300 to 700 W/m^2, and the temperature is at 45 °C. When $dP/dV < 0$, decreasing the reference voltage V_r forces dP/dV to approach zero; when $dP/dV > 0$, increasing the reference voltage V_r forces dP/dV to approach zero; when $dP/dV = 0$, V_r does not need any change. The flowchart is shown in Fig. 1(c). In Fig. 1(c), V_n and I_n are the momentary voltage and current of the PV array, while V_p and I_p are the previous voltage and current. When the PV array is operated at the maximum power point, the reference voltage is kept at a constant value, and thus oscillation is reduced.

III. System Configuration and Control

A traditional two-stage PV energy conversion system is connected between the PV array and the electrical power system [11]. The dc/dc converter is controlled so as to track the maximum power point of the PV array and to transfer energy to the batteries and inverter. The dc/ac inverter is controlled to produce

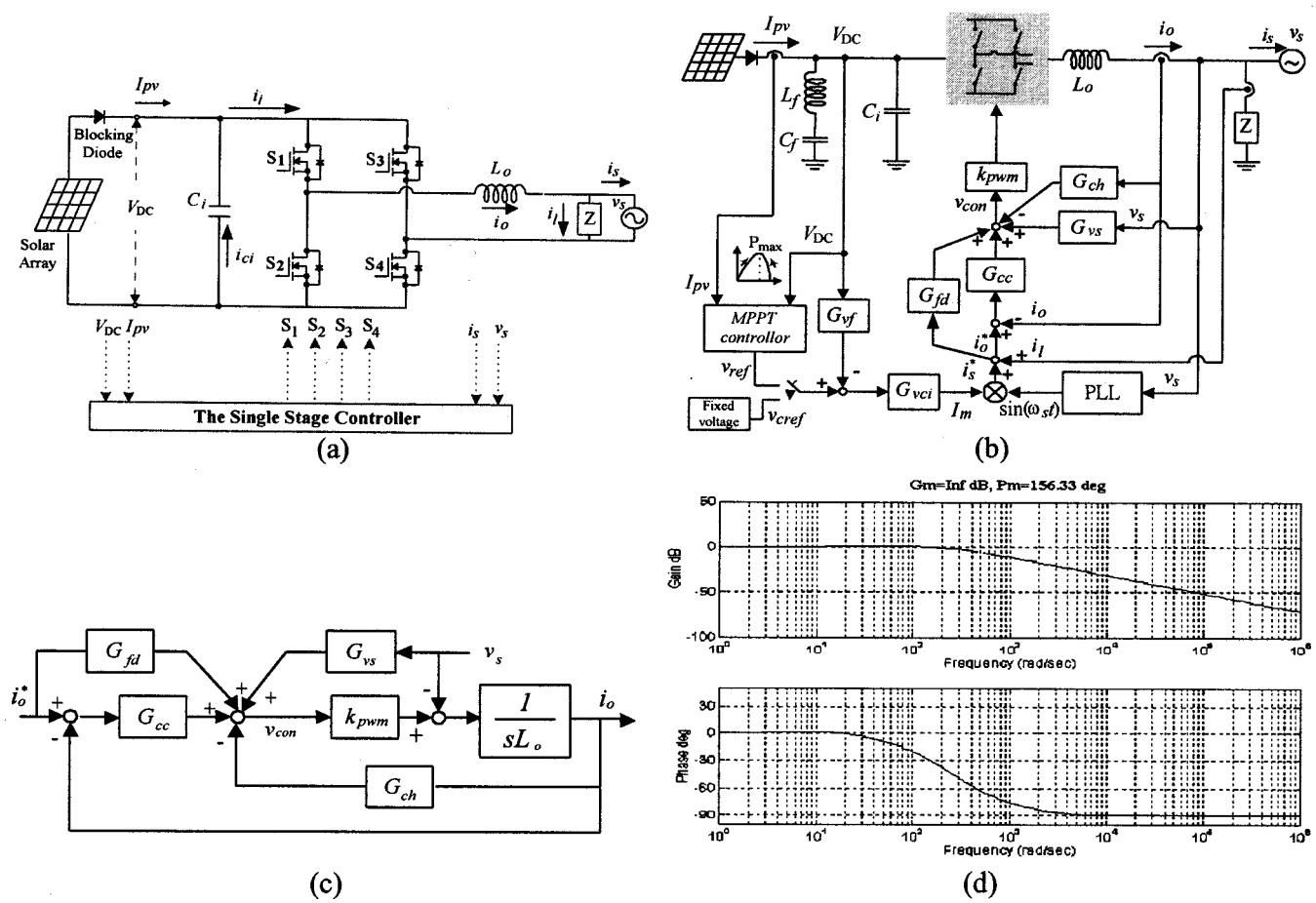

Fig. 2. Proposed photovoltaic energy conversion system. (a) Architecture. (b) Controller diagram. (c) Block diagram of current loop. (d) Bode diagram.

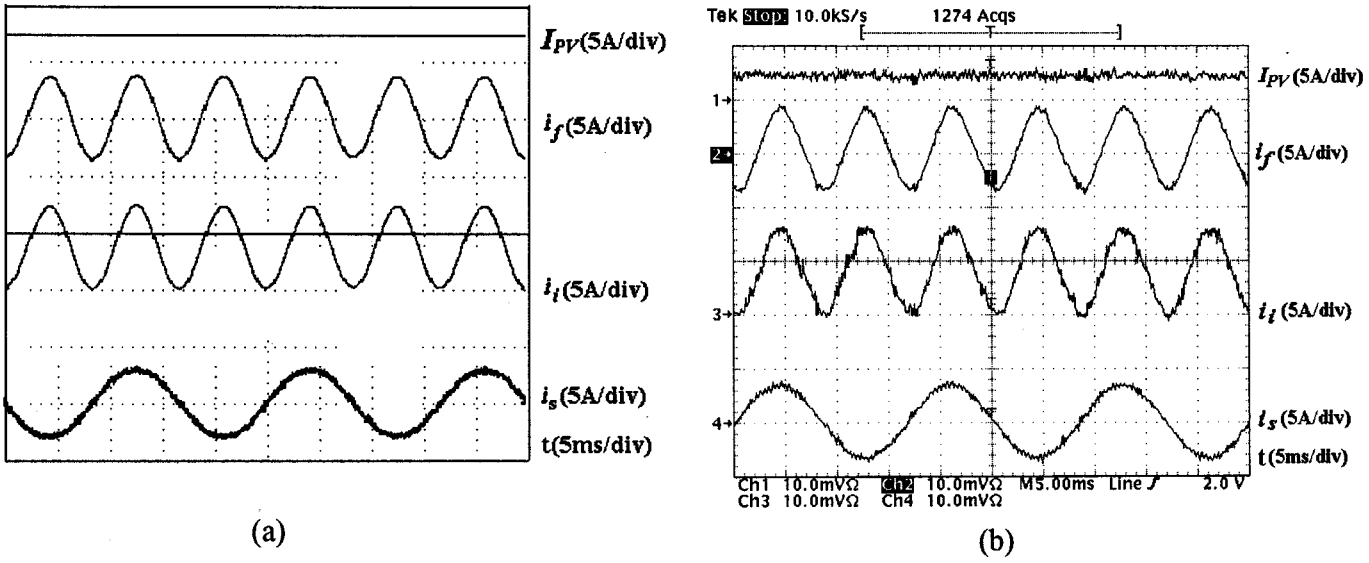

Fig. 3. Input and output current of the proposed conversion system. (a) Simulated result. (b) Experimental result.

an output current in phase with the utility voltage and to obtain a unity power factor. Because the dc/dc converter and the dc/ac inverter have independent control architecture, the controllers are easy to design. Yet, the efficiency of the entire conversion system is low because of the dc/dc converter, batteries, and dc/ac inverter.

The system configuration of a single-stage PV energy conversion system is shown in Fig. 2(a). The single-stage PV energy conversion system is controlled so as to supply power to the load and supply surplus power with a unity power factor to the utility line. Simultaneously, the single-stage conversion system must be operated so as to track the maximum power point of the

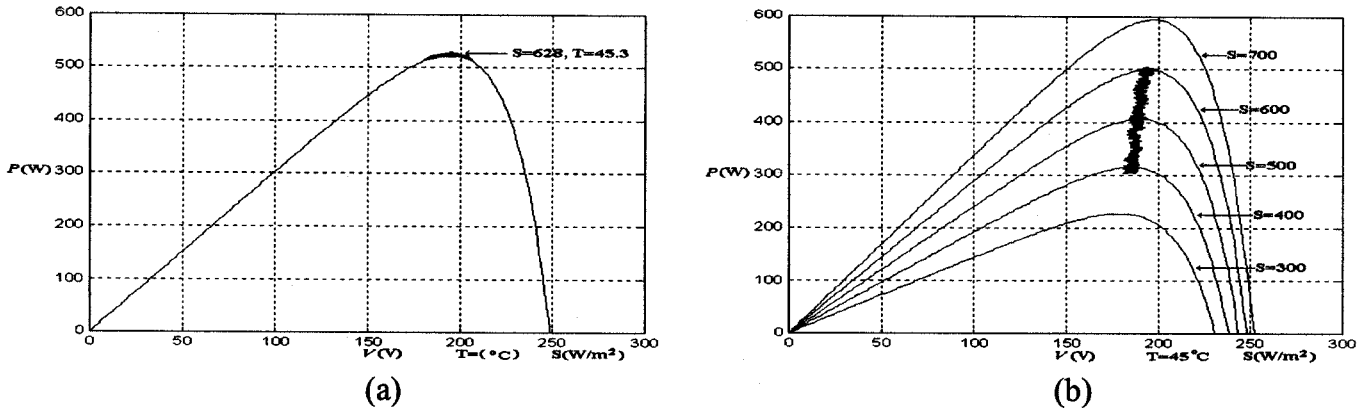

Fig. 4. MPPT measurement of the perturbation and observation method. (a) Constant insolation. (b) Varying insolation.

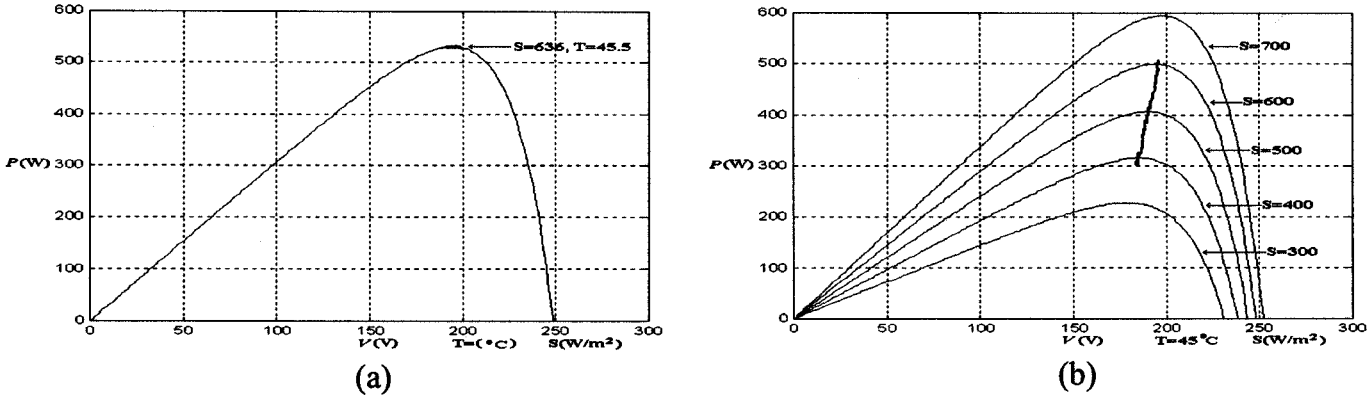

Fig. 5. MPPT measurement of the proposed method. (a) Constant insolation. (b) Varying insolation.

PV array. Thus, controller design of the single-stage configuration is more difficult than the two-stage configuration. Fig. 2(b) shows the controller block diagram of the proposed single stage system in which an 89c51 microprocessor is used for maximum power-point tracking. When the system is operated in the solar generator mode, the single-stage MPPT controller is used to compute the v_{ref} according to the proposed MPPT algorithm. When the system is operated in the active power line conditioner mode, the reference voltage is a constant voltage. The voltage controller G_{vci} is used to control the voltage loop to produce the dc reference current command I_m. Then, the dc reference current is multiplied by $\sin\omega_s t$, which is captured from the phase-locked-loop (PLL) circuit to produce the ac reference current command i_s^*. i_s^* is added to the load current i_l in order to produce the reference output current command i_o^* of the inverter. The differential equation of the inverter is

$$L_o \frac{di_o}{dt} = k_{\rm pwm} v_{\rm con} - v_s \tag{6}$$

where

$$k_{\rm pwm} = \frac{V_{DC}}{v_{\rm tri}} \tag{7}$$

and L_o is the output inductor of the inverter, i_o is the output current of the inverter, $v_{\rm DC}$ is dc-bus voltage, $v_{\rm tri}$ is the peak of the triangular carrier signal, $v_{\rm con}$ is the control signal which shapes the sinusoidal current to the utility line and also adjusts

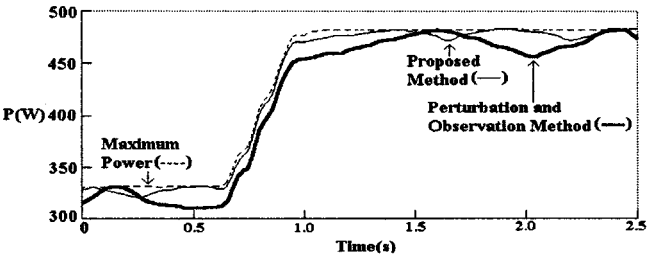

Fig. 6. Solar array output power of the proposed method and the perturbation and observation method.

system parameters for MPPT, and v_s is the utility voltage. Error e is defined as

$$e = i_s^* - i_s. \tag{8}$$

Because a perfect sinusoidal current to the utility line is a design goal, e must naturally approach zero. Thus,

$$\frac{de}{dt} = \frac{di_s^*}{dt} - \frac{di_s}{dt} \tag{9}$$

$$= \frac{di_s^*}{dt} + \frac{di_l}{dt} - \frac{di_o}{dt}. \tag{10}$$

From (6),

$$\frac{di_o}{dt} = \frac{1}{L_o}\left(k_{\rm PWM} v_{\rm con} - v_s\right). \tag{11}$$

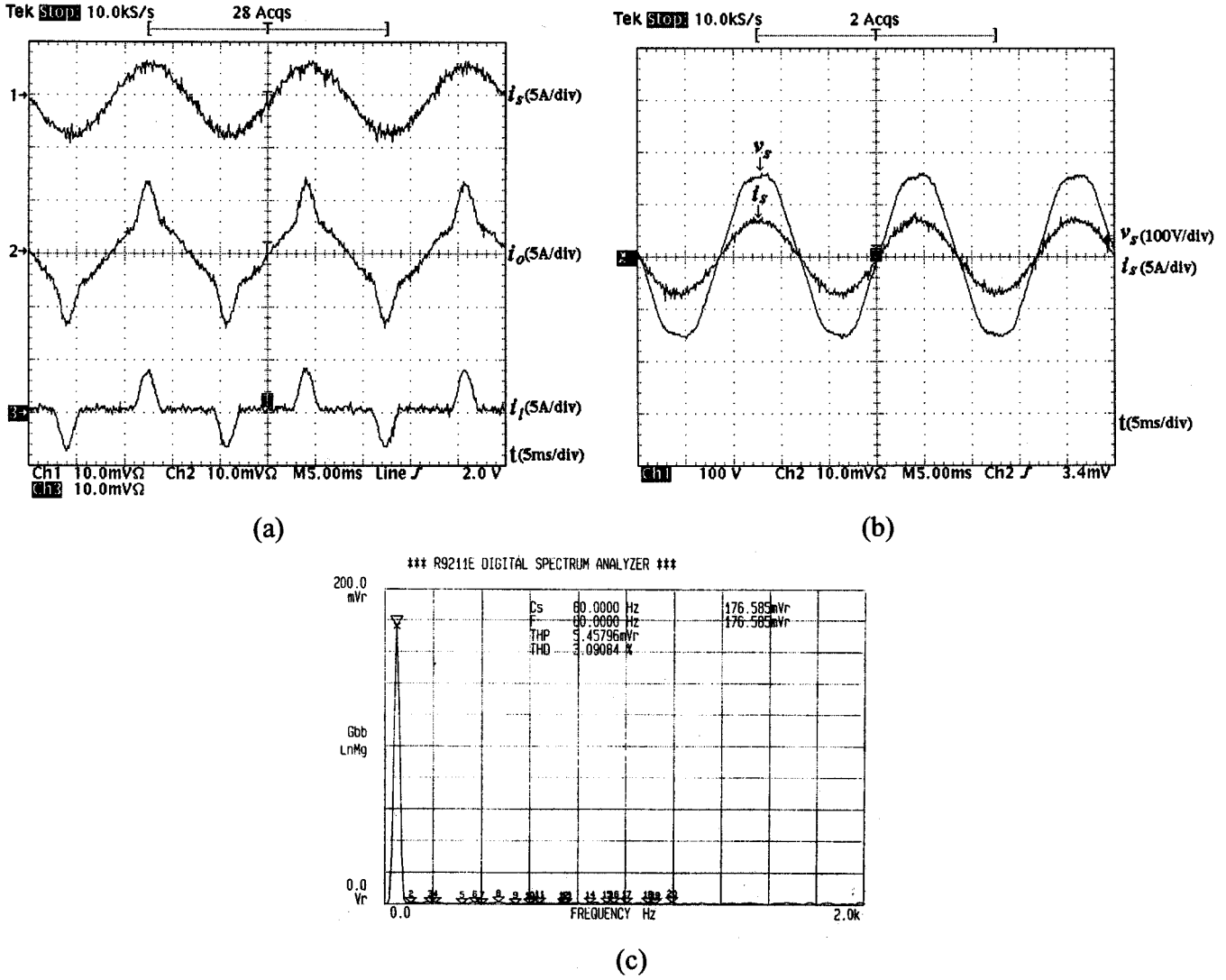

Fig. 7. Solar generator mode. (a) Waveforms of i_s, i_o, and i_l. (b) Waveforms of v_s and i_s. (c) Current spectrum of i_s.

Substituting (11) into (10) gives

$$\frac{de}{dt} = \frac{di_s^*}{dt} + \frac{di_l}{dt} + \frac{1}{L_o} v_s - \frac{1}{L_o} k_{\mathrm{PWM}} v_{\mathrm{con}} = 0. \tag{12}$$

Thus,

$$v_{\mathrm{con}} = \frac{1}{k_{\mathrm{PWM}}} L_o \left(\frac{di_s^*}{dt} + \frac{di_l}{dt} \right) + \frac{1}{k_{\mathrm{PWM}}} v_s \tag{13}$$

$$= \frac{1}{k_{\mathrm{PWM}}} L_o \frac{di_o^*}{dt} + \frac{1}{k_{\mathrm{PWM}}} v_s. \tag{14}$$

From (14), it is seen that v_{con} is composed of two terms. The first term is used to obtain a fast current control effect for i_o^*. The second term is used to compensate the disturbance from the utility voltage. In the first term, because a pure differential control tends to induce a large amount of noise in experimental implementation, a fast current loop is used instead. Feedforward controller G_{fd}, feedback-compensated controller G_{ch}, and phase-lead controller G_{cc} are used to get a fast current response in the current loop. The utility voltage disturbance controller G_{vs} is used to reduce the disturbed voltage component. Filter G_{vf} is used to produce feedback signals to the voltage loop. From Fig. 2(c), it can be seen that

$$i_o = \frac{k_{\mathrm{pwm}}(G_{fd} + G_{cc})}{sL_o + k_{\mathrm{pwm}}(G_{ch} + G_{cc})} i_o^* + \frac{k_{\mathrm{pwm}} \left(G_{vs} - \dfrac{1}{k_{\mathrm{pwm}}} \right)}{sL_o + k_{\mathrm{pwm}}(G_{ch} + G_{cc})} v_s. \tag{15}$$

From (15), when $G_{vs} = 1/k_{\mathrm{pwm}}$, the disturbance from v_s can be eliminated. If $|j\omega L_o| \ll |k_{\mathrm{pwm}}(G_{ch} + G_{cc})|$ and $G_{fd} = G_{ch}$, then $i_o/i_o^* \cong 1$, identifying accurate current control effect for i_o^*. The transfer functions of the controller are represented as follows:

$$G_{vci} = k_{vcp} + \frac{k_{vci}}{s} \tag{16}$$

$$G_{fd} = \frac{\tau_{cz3} s}{\tau_{cp3} s + 1} \tag{17}$$

$$G_{ch} = \frac{\tau_{cz2} s}{\tau_{cp2} s + 1} \tag{18}$$

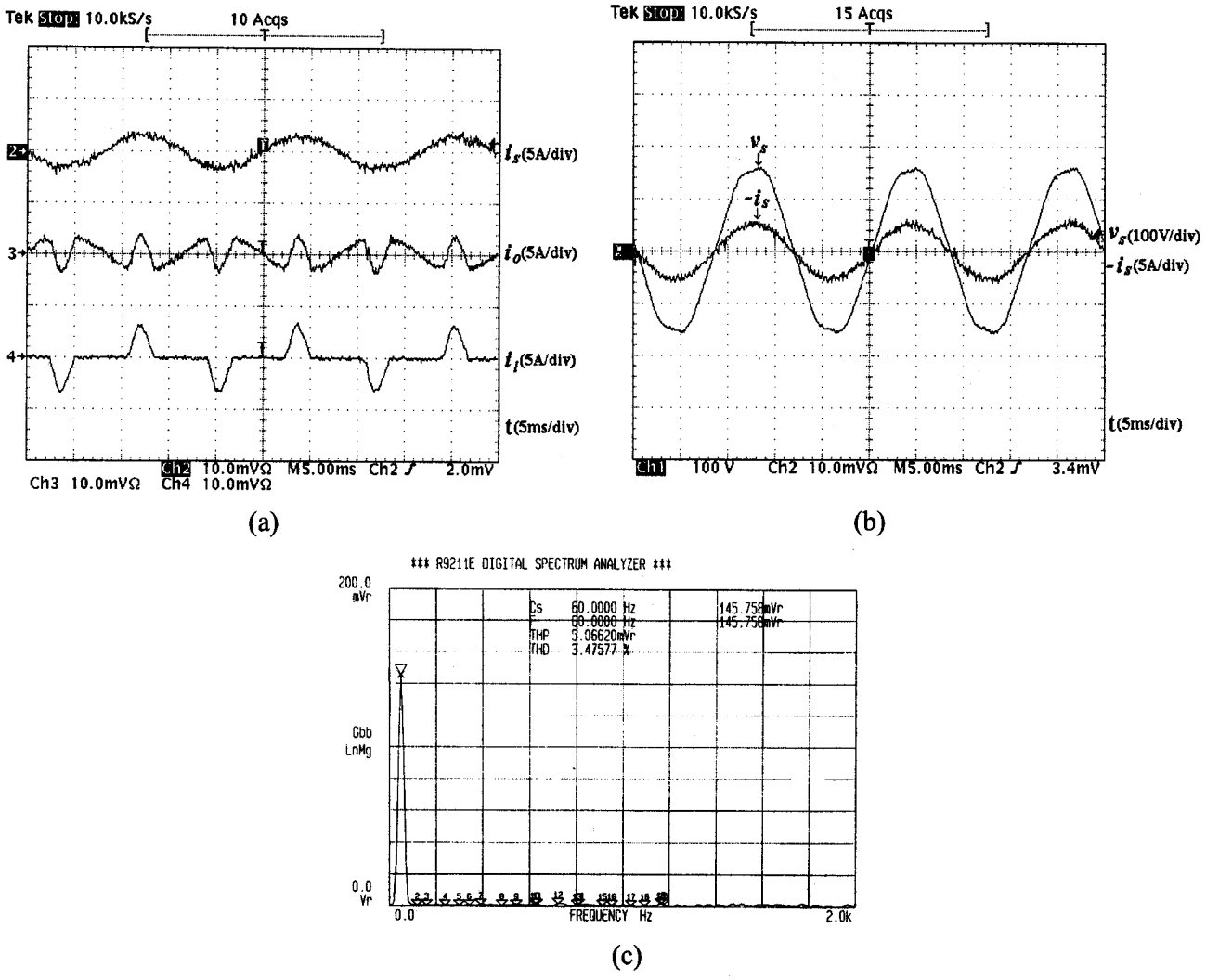

Fig. 8. Active power line conditioner mode. (a) Waveforms of i_s, i_o, and i_l. (b) Waveform of v_s and $-i_s$. (c) Current spectrum of i_s.

$$G_{cc} = k_{cp} + k_{cc}\frac{1}{\tau_{cp1}s+1} \tag{19}$$

$$G_{vs} = \frac{1}{k_{\text{pwm}}} \tag{20}$$

$$G_{vf} = \frac{k_{vf}}{1+s\tau_{vfp}}. \tag{21}$$

The Bode diagrams of the proposed system are shown in Fig. 2(d).

IV. Experimental and Simulated Results

Generally speaking, the frequency of the inverter input current is twice the fundamental frequency of the inverter output current [8]. Thus, a large capacitor must be connected with the PV array output to supply the low-frequency component of the inverter input current. In the proposed system, a series *LC* filter is connected with the PV array output to share the responsibility. From Fig. 2, the impedance of the *LC* filter is

$$Z_f = sL_f + \left.\frac{1}{sC_f}\right|_{S=j\omega} = j\left(\omega L_f - \frac{1}{\omega C_f}\right). \tag{22}$$

If

$$\omega = 2\omega_s = \frac{1}{\sqrt{L_f C_f}}, \qquad \text{then } Z_f = 0. \tag{23}$$

According to (22) and (23), L_f and C_f are chosen to support the inverter input current. The simulated and experimental results of Fig. 3 verify that the *LC* filter supports the second-order component current, where i_i is the inverter input current, i_{pv} is the output current of the PV array, i_f is the filter current, and i_s is the current fed from the PV energy conversion system to the utility line. From equations (22) and (23), Z_f supplies the second-order harmonic component, so the dc-bus capacitor supports only the components larger or equal to the fourth-order harmonic. Thus, the volume of the capacitor can be reduced.

To verify the performance of the proposed PV energy conversion system, the following parameters are selected for experimental implementation.

- *14 PV array modules*
  PV array specifications:
  rated power = 1050 W, rated current = 4.4 A;
  rated voltage = 238 V, short-circuit current = 4.8 A;
  open-circuit voltage = 308 V, temperature = 25 °C;

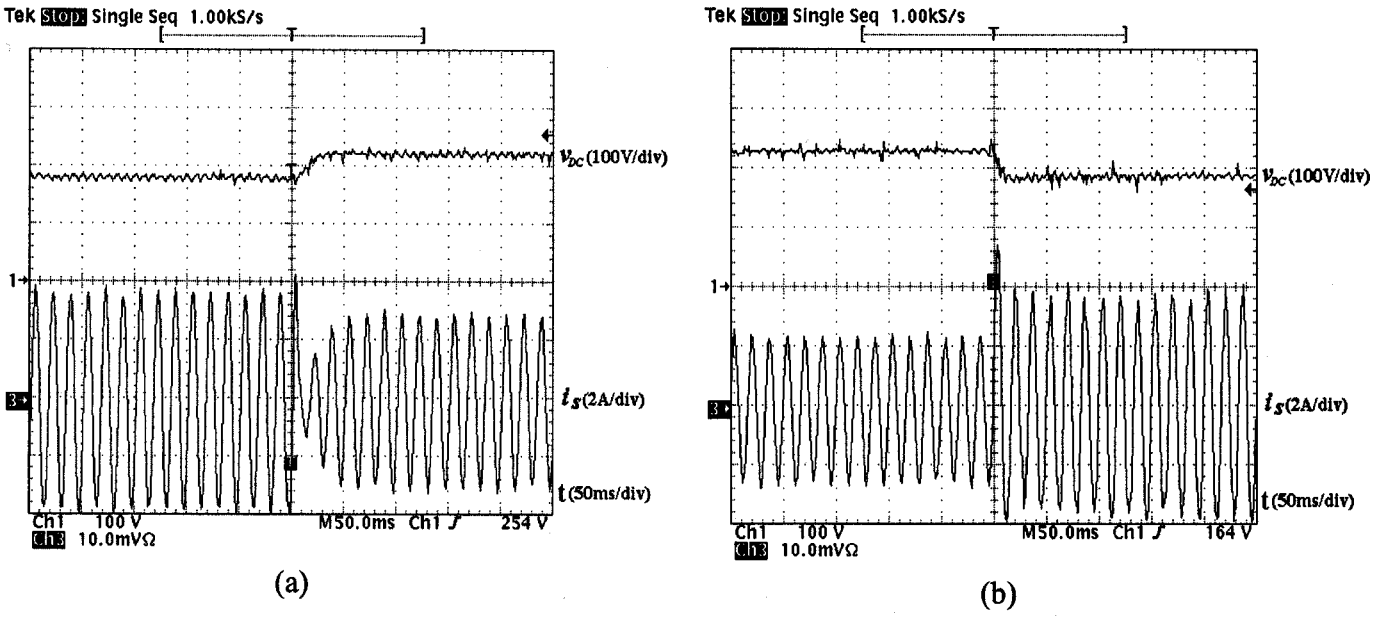

Fig. 9. Waveforms of $v_{\rm DC}$ and i_s. (a) From solar generator mode to active power line conditioner mode. (b) From active power line conditioner mode to solar generator mode.

- *output voltage:* 110 V, 60 Hz;
- *load:* rectifier load 300 W;
- *inverter switching frequency:* 18 kHz;
- *input filter capacitor:* $C_i = 470\ \mu$F;
- *LC series filter:* $L_f = 1.66$ mH, $C_f = 1000\ \mu$F;
- *output filter inductor:* $L = 1.2$ mH
- *converter component:* $S_1 \sim S_4$ (MOSFET) IRFP460;
- *blocking diode:* D_i: 6A600V×2;
- *voltage controller parameters:* $k_{vcp} = 3$, $k_{vci} = 50$, $k_{vf} = 0.01$, $\tau_{vfp} = 0.000\,16$;
- *current controller parameters:* $k_{cp} = 50$, $k_{cc} = 7.556$, $\tau_{cp1} = 0.102$, $\tau_{cp2} = 0.068$, $\tau_{cp3} = 0.068$, $\tau_{cz2} = 1.2132$, $\tau_{cz3} = 1.2132$.

The proposed PV energy conversion system provides two functions: 1) on sunny days, the PV array outputs power to the load and to the utility line, with a unity power factor and 2) when the PV array cannot supply enough power to the load, the conversion system is operated as active power line conditioner. The experimental results are discussed as follows.

1) *Solar Generator Mode (Sunny Day):* Fig. 4 shows the MPPT measurement diagram using the perturbation and observation method with constant and varied insolation and temperature. Serious oscillation can be observed. Fig. 5 shows the MPPT measurement diagram using the proposed MPPT algorithm. Oscillation is clearly reduced, providing experimental proof that the proposed method can track the maximum power point better than the perturbation and observation method. Fig. 6 shows the comparison of the solar array output power. From the result, the proposed method is better than the perturbation and observation method in the output power and response speed. The increase in output power is 2.4%, and the decrease in response time is 33%. Fig. 7(a) shows the i_s, i_o, and i_l current waveforms. Fig. 7(b) is the utility line voltage and the current fed from the PV energy conversion system to the utility line, showing that the current is sinusoidal and in phase with the utility voltage. Fig. 7(c) is the output current spectrum of i_s, showing a total harmonic distortion (THD) of 3.09%.
2) *Active Power Line Conditioner Mode (Low Insolation):* Fig. 8 depicts line current $-i_s$, a sinusoidal waveform in phase with the utility voltage. The THD of i_s is 3.48%. Fig. 9 shows the proposed conversion system switching between solar generator mode and active power line conditioner mode. Despite the rapid switch, system behavior is stable, indicating that the transient state response is excellent, and that the conversion system provides smooth and stable operation. Fig. 10 shows the efficiency of the proposed conversion system, which is higher than 90%.

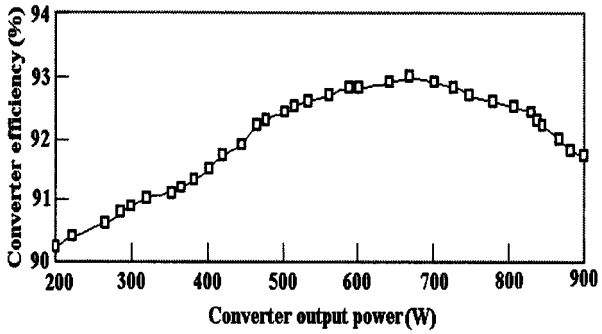

Fig. 10. Efficiency of the proposed conversion system.

V. Conclusions

Conventional two-stage PV energy conversion systems are bulky, expensive, provide low efficiency, and are, thus, not suitable for small-scale PV energy conversion utilization. To resolve this problem, a PV energy conversion system with single-stage architecture has been presented. The proposed

single-stage system has advanced features such as small physical volume, low weight, and high efficiency. A novel single-stage MPPT controller is used for rapid tracking of the PV array's maximum power point. The proposed algorithm reduces oscillation, resulting in significantly improved tracking. The proposed PV energy conversion system operates in two modes, providing solar generation when insolation is adequate and active power line conditioning when insolation is inadequate. Switching between the two modes is smooth and stable. The excellent performance of the proposed system is verified from both simulated and experimental results.

REFERENCES

[1] J. H. R. Enslin, M. S. Wolf, D. B. Snyman, and W. Sweigers, "Integrated photovoltaic maximum power point tracking converter," *IEEE Trans. Ind. Electron.*, vol. 44, pp. 769–773, Dec. 1997.

[2] T. Hiyama, S. Kouzuma, and T. Imakubo, "Identification of optimal operation point of PV modules using neural network for real time maximum power tracking control," *IEEE Trans. Energy Conversion*, vol. 10, pp. 360–367, June 1995.

[3] ——, "Evaluation of neural network based maximum power tracking controller for PV system," *IEEE Trans. Energy Conversion*, vol. 10, pp. 543–548, Sept. 1995.

[4] J. Applebaum, "The quality of load matching in a direct-coupling photovoltaic system," *IEEE Trans. Energy Conversion*, vol. EC-2, pp. 534–541, Dec. 1987.

[5] S. M. Alghuwainem, "Matching of a DC motor to a photovoltaic generator using a step-up converter with a current locked loop," *IEEE Trans. Energy Conversion*, vol. 9, pp. 192–198, Mar. 1994.

[6] M. M. Saied, A. A. Hanafy, M. A. El-Gabaly, and A. M. Sharaf, "Optimal design parameter for a PV array coupled to a DC motor via a DC–DC transformer," *IEEE Trans. Energy Conversion*, vol. 6, pp. 593–598, Dec. 1991.

[7] I. H. Altas and A. M. Sharaf, "A novel on-line MPP search algorithm for PV arrays," *IEEE Trans. Energy Conversion*, vol. 11, pp. 748–754, Dec. 1996.

[8] B. K. Bose, P. M. Szczeny, and R. L. Steigerwald, "Microcomputer control of a residential photovoltaic power conditioning system," *IEEE Trans. Ind. Applicat.*, vol. IA-21, pp. 1182–1191, Sept./Oct. 1985.

[9] C. Hua, J. Lin, and C. Shen, "Implementation of a DSP-controlled photovoltaic system with peak power tracking," *IEEE Trans. Ind. Electron.*, vol. 45, pp. 99–107, Feb. 1998.

[10] K. H. Hussein, I. Muta, T. Hoshino, and M. Osakada, "Maximum photovoltaic power tracking: An algorithm for rapidly changing atmospheric conditions," *Proc. IEE—Generation, Transmission, Distribution*, vol. 142, no. 1, pp. 59–64, Jan. 1995.

[11] S. J. Chiang, K. T. Chang, and C. Y. Yen, "Residential energy storage system," *IEEE Trans. Ind. Electron.*, vol. 45, pp. 385–394, June 1998.

[12] C. C. Hua and J. R. Lin, "DSP-based controller application in battery storage of photovoltaic system," in *Proc. IEEE IECON'96*, vol. 3, 1996, pp. 1705–1710.

[13] S. Nonaka and Y. Neda, "Single phase composite PWM voltage source," in *Conf. Rec. IEEE-IAS Annu. Meeting*, 1994, pp. 761–767.

Yeong-Chau Kuo was born in Tainan, Taiwan, R.O.C., in 1966. He received the B.S. and M.S. degrees in electrical engineering in 1990 and 1992, respectively, from National Taiwan Institute of Technology, Taipei, Taiwan, R.O.C. He is currently working toward the Ph.D. degree at National Cheng Kung University, Tainan, Taiwan, R.O.C.

His research interests are power electronics and control systems.

Tsorng-Juu Liang (M'93) was born in Kaohsiung, Taiwan, R.O.C. He received the B.S. degree in electrophysics from National Chiao-Tung University, Hsinchu, Taiwan, R.O.C., and the M.S. and Ph.D. degrees in electrical engineering from the University of Missouri, Columbia, in 1985, 1990, and 1993, respectively.

From June 1987 to May 1989, he was a Research and Design Engineer with TECO Electric and Machinery Company, Taiwan, R.O.C., working on switching-mode power-supply design. From 1990 to 1993, he was a Research Assistant in the Power Electronics Research Center, University of Missouri. From 1993 to 1998, he was with Kaohsiung Polytechnic Institute as an Associate Professor of Electrical Engineering. In 1998, he joined the Department of Electrical Engineering, National Cheng Kung University, Tainan, Taiwan, R.O.C., where he is currently an Assistant Professor. His research interests are in power electronics, including inverters, UPSs, electronic ballasts, resonant converters, and power-factor correction.

Dr. Liang is a member of the IEEE Industrial Electronics, IEEE Power Electronics, and IEEE Industry Applications Societies.

Jiann-Fuh Chen (S'79–M'80) was born in Chung-hua, Taiwan, R.O.C., in 1955. He received the B.S., M.S., and Ph.D. degrees in electrical engineering from National Cheng Kung University, Tainan, Taiwan, R.O.C., in 1978, 1980, and 1985, respectively.

Since 1980, he has been with the Department of Electrical Engineering, National Cheng Kung University, where he is currently a Professor. His research interests are power electronics and energy conversion.

Dr. Chen is a member of the IEEE Power Electronics Society.